Proceedings of the ASME 2012 31st International Conference on Ocean, Offshore and Arctic Engineering
OMAE2012
July 1-6, 2012, Rio de Janeiro, Brazil

OMAE2012-83729

DEVELOPMENT OF AN ON-BOARD WAVE ESTIMATION SYSTEM BASED ON THE MOTIONS OF A MOORED FPSO: COMMISSIONING AND PRELIMINARY VALIDATION

Alexandre N. Simos
Numerical Offshore Tank (TPN)
University of São Paulo
São Paulo,SP, Brazil

Eduardo A. Tannuri
Numerical Offshore Tank (TPN)
University of São Paulo
São Paulo,SP, Brazil

José J. da Cruz
Automation and Control Lab.
University of São Paulo
São Paulo,SP, Brazil

Asdrubal N. Queiroz Filho
Numerical Offshore Tank (TPN)
University of São Paulo
São Paulo,SP, Brazil

Iuri B . da Silva Bispo
Numerical Offshore Tank (TPN)
University of São Paulo
São Paulo,SP, Brazil

Rafaella C. A. Carvalho
Petrobras E&P
Rio de Janeiro, RJ, Brazil

ABSTRACT

This paper addresses the development, installation and initial tests of a system for wave spectra estimation from the measurements of the first order motions of a moored FPSO located in Campos Basin, Brazil. The estimation is based on Bayesian inference algorithms, previously validated by means of numerical and small-scale experimental analysis. A 6-dof inertial measurement unit (IMU) is used for monitoring the motions of the platform, and this information is sent to a remote data-base, also accessed by the wave-estimation system. The algorithm also requires the Response Amplitude Operators (RAOs), and they depend on the loading conditions of the FPSO.

A previous analysis considering typical loading configurations of the tanks showed that the wave estimation is mainly dependent on the total displacement of the vessel, and not on the load distribution among the tanks. Hence, the RAOs for the full-range of drafts (or total displacements) were numerically generated, considering a uniform distribution of the load among the tanks. Since the draft of the platform was not directly measured, the loading levels of the tanks are obtained from the automation system of the platform, and the draft is then estimated. Finally, the heading is measured by a gyrocompass, and it is necessary for the definition of the global wave direction. The Bayesian estimation is executed at time-spans of 30min. A parametric optimization algorithm is then applied for the calculation of the wave spectrum parameters from the raw-spectrum obtained by the Bayesian estimation.

A user-friendly interface was also developed, with on-line information about platform motions, estimated wave spectrum, peak statistics and data history. Since all information is accessed by network, the wave system can be installed either on-board or in the on-shore monitoring center.

The system was commissioned and a partial 3-month validation campaign was executed. The spectrum results were compared to NOAA estimates. As expected, low-period wave components (smaller than 8s) could not be estimated with accuracy, since the FPSO presents small motion response for these components. Swell and high-period wave components estimates presented good qualitative and quantitative agreement with satellite prediction.

KEYWORDS

Wave spectra, Bayesian estimation, FPSO, 6-dof inertial movement.

INTRODUCTION

Considerable effort has been dedicated to develop good-quality wave estimates from the record of vessels' motions by several research groups (see for example Iseki and Ohtsu [1], Nielsen [2] and Simos et al. [3])

When compared to other wave monitoring systems, such as buoys or radar systems, the main advantage that arises from this method concerns the simplicity of the instrumentation (composed basically of accelerometers and rate-gyros), which is very easy to install on-board and, furthermore, requires a rather uncomplicated maintenance, especially if compared to the wave buoys. On the other hand, the limitation is also clear: only waves that impose a reasonable level of motion may be inferred. In other words, the vessel acts as a low-pass filter,

filtering the high frequency components that do not excite the vessel's first-order response. That is the main reason why this kind of methodology cannot be envisaged as a substitute for wave buoys for the sake of long-term oceanographic records. It may, however, provide important information concerning the operation of such vessels when the problems are directly connected to the waves in the range of frequencies that do impose significant motions to the floating unit.

The filter analogy also indicates that the range of frequencies for which the spectrum can be estimated will depend decisively on the size of the vessel. Large-displacement vessels, such as the VLCCs on which the FPSOs are usually based, will have lower cut-off frequencies if compared to smaller vessels, such as a crane-barge.

This paper addresses the development, installation and initial tests of the system for wave spectra estimation from the measurements of the first order motions of a moored FPSO located in Campos Basin, Brazil. It is a natural continuation of the research conducted at University of São Paulo in cooperation with Petrobras for more than 10 years. Previous validations were based on small scale experiments ([3],[4]) and a short-term real-scale campaign [5].

The main objective of this project is to develop a software package, integrated with the automation system of the platform, and to perform a long-term validation campaign. The input to the software include the motions, the heading and the draft of the ship. Since all the tests addressed in this paper were made using a spread-moored FPSO located in Campos Basin, Brazil, from now on it is considered that the system is prepared for FPSO systems. However, any customization for other types of vessels may be done with few engineering hours.

The next section presents an overview of the system, considering hardware integration and software structure. After that, the wave estimation algorithms are detailed, including the procedure adopted to calibrate the Bayesian model, that involves the evaluation of the so-called hyperparameters. The requirements for the user interface were defined by the Oceanographic Group of Petrobras, and it is also presented. Finally, the results of the validation campaign are discussed by means of two illustrative examples.

SYSTEM DESCRIPTION

The FPSO already had an inertial measurement unit (IMU) and 6-dof motion data were available in a network database. Since the draft is not measured directly, the wave estimation software receives online data of the FPSO's cargo and ballast tanks and, based on the loading capacity plan of the vessel, performs a estimation of the draft. The Figure 1 shows the block diagram of the wave estimation system used in the FSPO.

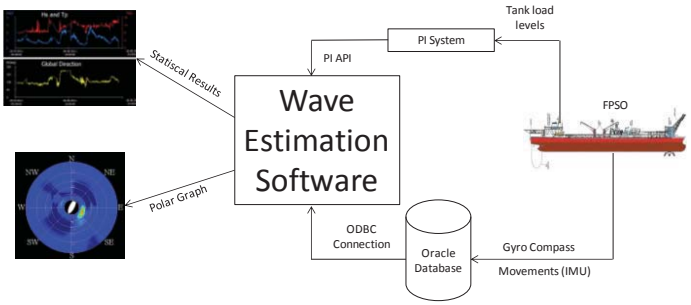

Figure 1 – Wave estimation system's diagram block

The wave estimation software can be defined in a few blocks as shown in Figure 2.

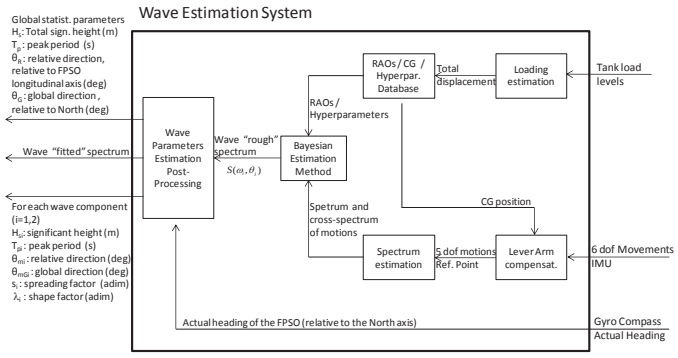

Figure 2 – Wave estimation software's diagram block

The loading estimation block estimates the FPSO's draft, receiving as input the tank loading levels. The draft is used by the next block to obtain the FPSO's response amplitude operators (RAO), the corresponding hyperparameters and the position of the center of gravity (CG). The spectrum estimation block computes the vessel motion's spectra and cross-spectra that will be used by the following block, the Bayesian Estimator. The wave spectrum is then estimated, and a post-processing block computes the wave statistics such as significant wave height, peak period and direction. These last two blocks will be discussed in the next section.

For an easy use and data visualization, a Graphical User Interface (GUI) was developed. The GUI also provides all the necessary software configuration in an easy way, such that all configuration parameters can be readily accessed and configured. The GUI will be presented in the Graphical Interface section.

ALGORITHM

Wave spectrum is estimated from the motion records by means of a Bayesian inference method, originally proposed by Iseki and Ohtsu [1] and later refined by Nielsen [2]. The method that is employed in this paper follows closely the one proposed by Nielsen, except for the set of motions that is adopted as input for the estimations: the roll motion is disregarded here due to the strong nonlinearities that affect the transfer function of this motion with respect to the incident

waves. The motions in the other five d.o.f. (surge, sway, heave, pitch and yaw) set the basis for the estimations discussed ahead.

The Bayesian estimation is based on the maximization of the product between the maximum likelihood function and a prior distribution, which represents the previous information regarding the unknown coefficients (in our case, the directional wave spectrum). The way that Bayes' theorem is applied in order to provide a useful mathematical algorithm for the motion-based wave estimation is well documented in literature and therefore will not be addressed here.

Ultimately, the inference method requires the minimization of the following functional:

$$J(\mathbf{x}) = \left|\mathbf{B} - \mathbf{A}\mathbf{x}\right|^2 + \mathbf{x}^T(u_1{}^2\mathbf{H}_1 + u_2{}^2\mathbf{H}_2 + u_3{}^2\mathbf{H}_3)\mathbf{x} \qquad (1)$$

In the expression above, **x** is the vector containing the unknown spectrum values for different wave frequencies $(\omega_m, m = 1,\ldots,M)$ and directions $(\theta_k, k = 1,\ldots,K)$:

$$\mathbf{x} = \begin{bmatrix} S(\omega_1,\theta_1) \\ S(\omega_1,\theta_2) \\ \vdots \\ S(\omega_M,\theta_{K-1}) \\ S(\omega_M,\theta_K) \end{bmatrix}$$

The vector **B** contains the values of the motion spectrum $\phi_{ii}(\omega_m)$ and cross-spectrum $\phi_{ij}(\omega_m)$ for the N different motions that are used as input (in this paper then, N=5). B is given by:

$$\mathbf{B} = [\mathbf{b_1} \quad \mathbf{b}_2 \quad \ldots \quad \mathbf{b}_M]^T, \text{ with } \mathbf{b_m} = \begin{bmatrix} \phi_{ii}(\omega_m) \\ \vdots \\ \mathrm{Re}[\phi_{ij}(\omega_m)] \\ \vdots \\ \mathrm{Im}[\phi_{ij}(\omega_m)] \\ \vdots \end{bmatrix} \qquad (2)$$

A is the $(N^2.M)\times(K.M)$ matrix that contains the dynamic characteristics of the vessel, expressed by means of its linear transfer functions of motion or RAOs. It can thus be written as:

$$\mathbf{A} = \begin{bmatrix} \mathbf{A_1} & \mathbf{0} & \cdots & \mathbf{0} \\ \mathbf{0} & \mathbf{A_2} & \cdots & \mathbf{0} \\ \vdots & \vdots & \ddots & \\ \mathbf{0} & \mathbf{0} & & \mathbf{A_M} \end{bmatrix} \qquad (3)$$

with 0 the $N^2 \times K$ zero matrix and

A_m=

$$\begin{bmatrix} |RAO_i(\omega_m,\theta_1)|^2 & \ldots & |RAO_i(\omega_m,\theta_k)|^2 & \ldots & |RAO_i(\omega_m,\theta_K)|^2 \\ & & \vdots & & \\ \mathrm{Re}(RAO_i(\omega_m,\theta_1)RAO_j(\omega_m,\theta_1)^*)\ldots & & \mathrm{Re}(RAO_i(\omega_m,\theta_k)RAO_j(\omega_m,\theta_k)^*) & \ldots & \mathrm{Re}(RAO_i(\omega_m,\theta_1)RAO_j(\omega_m,\theta_K)^*) \\ & & \vdots & & \\ \mathrm{Im}(RAO_i(\omega_m,\theta_1)RAO_j(\omega_m,\theta_1)^*)\ldots & & \mathrm{Im}(RAO_i(\omega_m,\theta_k)RAO_j(\omega_m,\theta_k)^*) & \ldots & \mathrm{Im}(RAO_i(\omega_m,\theta_1)RAO_j(\omega_m,\theta_K)^*) \\ & & \vdots & & \end{bmatrix}$$

The second term in equation (1) allows one to predefine different levels of smoothness of the estimated spectrum regarding its variation in frequency and direction and also avoids predicting spurious wave energy for frequencies outside the range of wave frequencies for which the vessel presents significant response.

Smoothness is controlled by means of the so-called hyperparameters $\{u_1, u_2\}$, in a way that can be easily understood: Assuming that the spectrum is smooth with respect to direction and frequency and defining the second order differences ε_{1mk} associated to direction k at frequency m and ε_{2mk} associated to the frequency m at the direction k as:

$$\begin{aligned} \varepsilon_{1mk} &= S(\omega_m,\theta_{k-1}) - 2S(\omega_m,\theta_k) + S(\omega_m,\theta_{k+1}) \\ \varepsilon_{2mk} &= S(\omega_{m-1},\theta_k) - 2S(\omega_m,\theta_k) + S(\omega_{m+1},\theta_k) \end{aligned}, \qquad (4)$$

the smoothness condition is equivalent to keeping the following summations as small as possible:

$$\begin{aligned} &\sum_{k=1}^{K}\sum_{m=1}^{M} \varepsilon_{1mk}{}^2 = \mathbf{x}^{\mathrm{T}}\mathbf{H_1}\mathbf{x} \quad \text{with } S(\omega_m,\theta_0) = S(\omega_m,\theta_K) \\ &\qquad\qquad \text{and } S(\omega_m,\theta_{K+1}) = S(\omega_m,\theta_1) \\ &\sum_{k=1}^{K}\sum_{m=2}^{M-1} \varepsilon_{2mk}{}^2 = \mathbf{x}^{\mathrm{T}}\mathbf{H}_2\mathbf{x} \end{aligned} \qquad (5)$$

where the matrixes $\mathbf{H_1}$ and $\mathbf{H_2}$ may be easily constructed considering the proper definition of the vector x (see, for example [2]). Thus, the hyperparameters $\{u_1, u_2\}$ operate in order to preset the level of smoothness desired in direction and frequency, respectively.

Furthermore, in order to avoid excessive spectral energy at the frequency boundaries, a third parameter is introduced. The reason why this is indeed necessary is clear: if the vessel has no significant response for a given wave frequency, then any amount of wave energy could be predicted in this range. In order to guarantee that this aspect has no significant influence on the estimated spectrum, the sum of the power of the spectrum is minimized in a pre-defined range of low and high frequencies given by $(\omega_1, \omega_2, \ldots, \omega_L, \omega_H, \ldots, \omega_M)$. Considering the discretization presented above, the following functional must be minimized (matrix $\mathbf{H_3}$ is obtained by a procedure similar to the one used to derive $\mathbf{H_1}$ and $\mathbf{H_2}$):

$$\sum_{k=1}^{K}\sum_{m=1}^{L} S(\omega_m,\theta_k)^{\,2} + \sum_{k=1}^{K}\sum_{m=H}^{M} S(\omega_m,\theta_k)^{\,2} = \mathbf{x}^{\mathrm{T}}\mathbf{H}_3\mathbf{x} \qquad (6)$$

Also, for avoiding spurious energy outside the range of frequencies with hull response (see eq. 6), the following limits

were adopted: ω_L=0.21rad/s and ω_H=0.79rad/s (values in real-scale, equivalent to wave periods of 30s and 8s, respectively). The RAOs of the FPSO confirm the small motion response for wave periods below 8s. For example, Figure 3 presents the heave RAO for a beam-incidence, considering three different loading conditions (full, ballasted and intermediate). The mooring system induces yaw low-frequency oscillations at periods of 30s or more, what justifies the value of ω_L adopted.

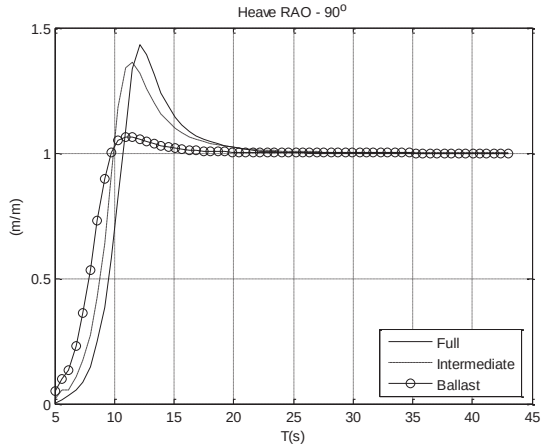

Figure 3 – Heave RAO of the FPSO

The number of directions (K) and frequencies (M) define the total size of the optimization problem, since the number of variables is K.M. In the present work, K=36 (10° intervals with respect to wave direction) and M=20 (considering a regular discretization in period, between 8s and 30s).

HYPERPARAMETERS DEFINITION

The problem that arises is that the three external hyperparameters must be predefined and, in principle, their values may change with the vessel characteristics (hull geometry, draft, inertial parameters, etc.) and also with respect to the incoming wave features (wave height, peak period, angle of incidence, etc.), which, of course, are unknown.

Many previous studies have shown that the usage of ABIC information criterion ([6], [7]) to evaluate the hyperparameters leads to high computational costs, making real time estimation impracticable. Also, results presented by Iseki [8] indicate that ABIC does not always provide the best values of u_1 and u_2, leading to errors on estimation, especially for wave direction estimates.

Fixed values of hyperparameters for each draft of the vessel were used by Simos et al. [3] and a sensibility analysis of estimates using a similar approach was made by Iseki and Nielsen [9]. However, this approach may lead to errors, since the hyperparameters should also vary with wave properties.

A sensibility analysis was carried out in order to verify whether or not the hyperparameters are dependent on observable quantities, such as peak period or vessels draft. This analysis was necessary to provide a practical scheme for on board wave spectrum estimation. The complete results of this analysis are presented in Bispo et al [10], and a brief summary is given below.

Numerical simulations of ship dynamics using a predefined set of wave conditions (significant wave height H_s, peak period T_p, direction θ_m and spread s) and vessel drafts were performed.

A grid of u_1 and u_2 was defined and for each pair of hyperparameters an iteration of the Bayesian algorithm was performed, using the series numerically generated for each combination of sea parameters and draft. The hyperparameter u_3 was not considered in the analysis, keeping a constant value.

Aiming to find tendencies on the values of the errors between theoretical and estimated spectra and to verify which of the parameters influenced the estimation the most, an error surface was created for the grid of hyperparameters (difference between exact and estimated wave spectra). Also, in each test, the pair of hyperparameters related to minimum error was considered as the optimum set. Figure 4 shows an example of such a surface.

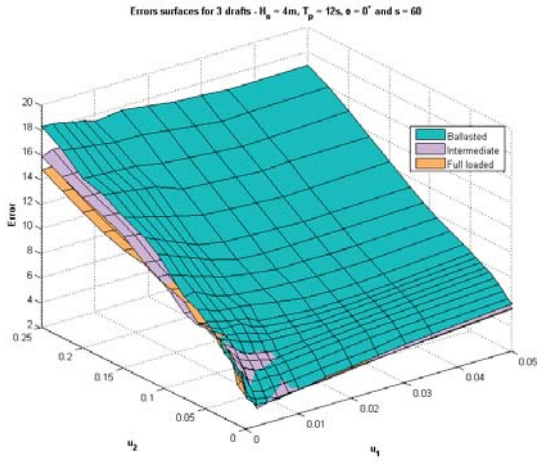

Figure 4 - Errors surfaces for $H_s = 4m$, $T_p = 12s$, $\theta = 0° = 0$ and $s = 60$ in three loading conditions.

Through the results of simulations and error surfaces, it was possible to observe that

- The draft, H_s and s parameters do not have significant influence on the choice of u_1 and u_2. The optimum hyperparameters were calculated for a typical H_s and s at Campos Basin, and for the intermediate draft of the FPSO.

- Wave direction plays an important role on the definition of the hyperparameters, but it is unknown *a priori*. However, it was verified that the optimum choice of the hyperparameters are more important for 0° or 180° wave incidence direction, when compared to near-beam sea incidence. In the later case, the wave estimate is more "robust", being less sensitive to the hyperparameters. So, u_1 and u_2 are defined considering 0° or 180° wave incidence direction.

- The peak period T_p has significant influence on the choice of u_1 and u_2. In order to simplify the dependency of the hyperparameters using measurable quantities, it is proposed the use of the average heave period (T_z) of the vessel, instead of the wave peak period, since, in general, they are stronlgy correlated.

So, the final methodology consisted on the pre-computation of the two hyperparameters (u_1 and u_2) as a function of the wave peak period. During the wave estimation, the average period of heave (T_z) is used as the input for obtaining the hyperparameters.

It was shown that this approach is better that considering fixed hyperparameters, and there is no significant error increase when compared to the utilization of "optimum" hyperparameters (meaning those that result in minimum error with respect to the theoretical wave spectrum) for each sea state and draft condition.

SPECTRUM PARAMETERS ESTIMATION

A JONSWAP model was used to provide estimates of sea parameters of crossed-sea spectra generated by the Bayesian algorithm. The general bi-modal (i=1,2) spectrum is given by:

$$S(\omega,\theta) = \frac{1}{4}\sum_{i=1}^{2} 2\pi\alpha_i \frac{g^2}{\omega^5} A(s_i)\cos^{2s_i}\left(\frac{\theta-\theta_{m_i}}{2}\right)\exp\left[\frac{-1.25\omega_{p_i}^4}{\omega^4}\right]\gamma_i^{\exp\left[-\frac{-(\omega-\omega_{p_i})^2}{2\sigma_i^2\omega_{p_i}^2}\right]}$$

where g is the gravity acceleration, ω_p is the peak frequency ($\omega_p = 2\pi/T_p$), s is the spreading factor. The parameter γ is a shape factor and σ is the peak width, given by:

$$\sigma = \begin{cases} 0.07 & \omega \le \omega_p \\ 0.09 & \omega > \omega_p \end{cases}$$

The term α is related to the significant height H_s, and to the peak frequency by:

$$\alpha = 5.0609\frac{H_s^2\omega_p^4}{(2\pi)^4}(1-0.0287\ln\gamma)$$

Function $A(s_i)$ is a normalization factor, given by:

$$A(s) = \frac{2^{2s-1}\boldsymbol{\Gamma}^{\mathbf{2}}(s+1)}{\pi\boldsymbol{\Gamma}(2s+1)}$$

However, using straight adjustment of bimodal JONSWAP model to the estimated $S(\omega,\theta)$ has shown to be not effective, since fitting of unimodal spectrum by a bimodal model leads to errors on second components of the spectral formulation. To outline this issue, a bimodality criterion was implemented using the formulation proposed by Piscopia et al. [11], so that one could previously distinguish a bimodal from a unimodal energy distribution of a given spectrum.

The authors proposed that the absolute difference (χ) of the overall mean direction (7) and the overall mean direction of the energy flux (8) should be greater than 3° for crossed-sea states and lower or equal otherwise. That work stresses that this threshold value was found based on the set of seas measured in the Mediterranean Sea.

$$\theta_m^L = \text{atan}\left[\frac{\int_0^\infty\int_0^{2\pi} S(f,\theta)\sin\theta d\theta df}{\int_0^\infty\int_0^{2\pi} S(f,\theta)\cos\theta d\theta df}\right] \qquad (7)$$

$$\theta_m^D = \text{atan}\left[\frac{\int_0^\infty\int_0^{2\pi} Cg(f)S(f,\theta)\sin\theta d\theta df}{\int_0^\infty\int_0^{2\pi} Cg(f)S(f,\theta)\cos\theta d\theta df}\right] \qquad (8)$$

where f is the frequency in Hz and $Cg(f)$ is the linear group velocity.

After defining which JONSWAP model should be used for fitting (uni or bimodal), an optimization routine is excecuted to find values of sea parameters in each case, using minimization of the error between $S(\omega,\theta)$ and the estimated JONSWAP spectrum at each iteration of the algorithm.

Such optimization routine is based on non-linear minimization algorithms, and convergence problems were verified in some cases. In order to obtain a more robust parametric estimation algorithm, the method proposed by Hanson and Phillips [12] will be implemented in the next version of the software.

GRAPHICAL INTERFACE

The graphical user interface (GUI) provided with the Bayesian estimation algorithm was designed for showing the main computed information in an easy way. Its main window (Figure 5) is basically divided into three sections: Statistics, Polar Graph and Movements.

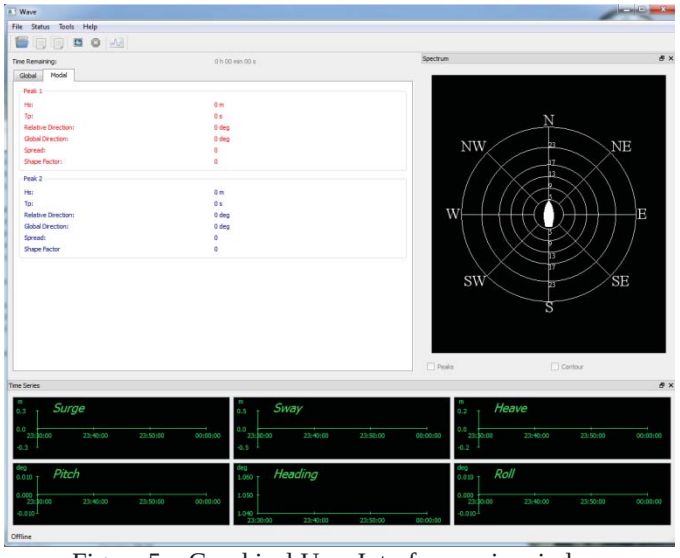

Figure 5 – Graphical User Interface main window

The Statistical section is shown in Figure 6 and is divided in two sub-sections: global and modal, which can be chosen by using the upper tab.

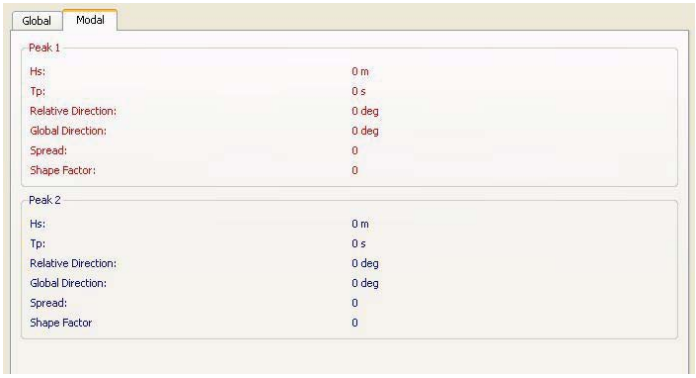

Figure 6 – GUI's Statistical section

In the "Global" tab are the global statistics such as significant wave height, peak period, global mean direction and relative direction. These global statistics are computed for the complete spectrum, ignoring if it has more than one energy peak. The global direction is relative to geographical North, while the relative direction is relative to the FPSO longitudinal axis, being 0^o for a stern incidence.

In the "Modal" tab, the parameters for each modal wave component are presented, including the spread and shape factors. For unimodal sea-states, peak 2 is not presented. In this case, global and modal statistics are the same.

Figure 7 shows the polar graph section. The polar graph shows the computed spectrum with a color map that ranges from dark blue (less energy) to red (peak energy) passing through green and yellow colors as the energy gets higher. The red arrow shows the modal direction relative to North. In the center of the polar graph there is drawing that indicates the heading of the FPSO obtained from the onboard gyro compass.

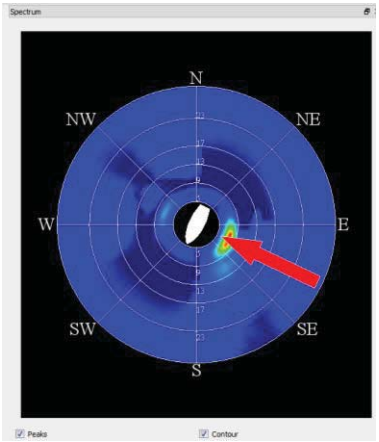

Figure 7 – GUI's polar graph

For bimodal sea states, the second peak direction is shown by a blue arrow. Both the color strength map and the arrows can be hidden by using the two selection boxes (contour and peaks respectively) under the polar graph.

The Movements section is shown in Figure 8. In this section the recorded FPSO's motions in 6 dof can be viewed. These motionss can be directly obtained from an IMU unity, from a database system or from an ASCII file (the two last options are not in real time). The movement acquisition modes will be discussed later in this section.

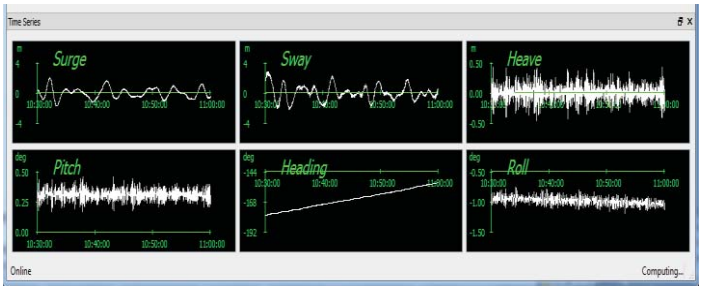

Figure 8 – GUI's movements time series

All the computed data (spectra and statistics) are saved in both binary and ASCII files. The binary file format is the HDF5 [12] which was chosen because of its many features such as data compression and hierarchical data storage. The input data is also saved but only in binary format and is used for later offline computation and calibration. For each wave estimation, one different ASCII file is saved, while a binary HDF5 file can contain as many estimations as produced in an entire week. The content of an ASCII file can be "viewed" from inside the GUI. To facilitate the data transmission, the GUI also includes a routine that converts the HDF5 file in many ASCII files. With this routine only the HDF5 file is necessary for recovering all computed data. Statistical time series can be obtained from the HDF5 file too, or can be directly plotted to a graph inside the GUI. Figure 9 shows the history of the statistics generated from an HDF5 file. The time period for the graphic is configurable by the user.

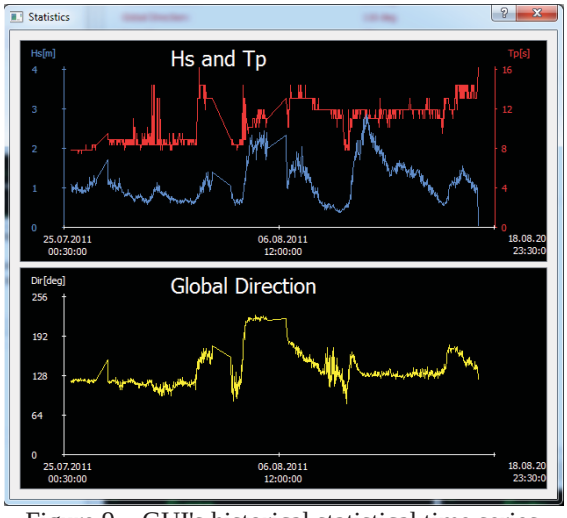

Figure 9 – GUI's historical statistical time series

The configuration parameters of the GUI can be found in the preferences window which can be accessed by the tool "menu". In this window (Figure 10) two tabs can be found. The input data configuration parameters are in the Data Source tab.

Data can be input from an ASCII file, from the PI system, from an Oracle database or directly from a IMU sensor connected in the serial port. If using the sensor mode, the serial port parameters must be configured.

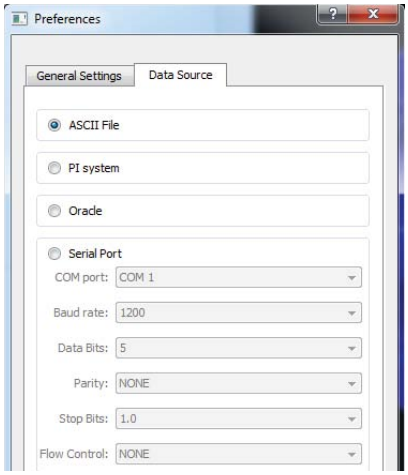

Figure 10 – Preferences window - data source tab

In the "General Settings" tab the Update Interval parameter sets the frequency of execution of the estimation algorithm. In the time series group, the display parameter sets the time shown in the time series section. There are also 6 check boxes, that define which motions are shown in the time series section of the main window. The time parameter sets the length of dataset to be used by the wave estimation algorithm. The default value is 30min.

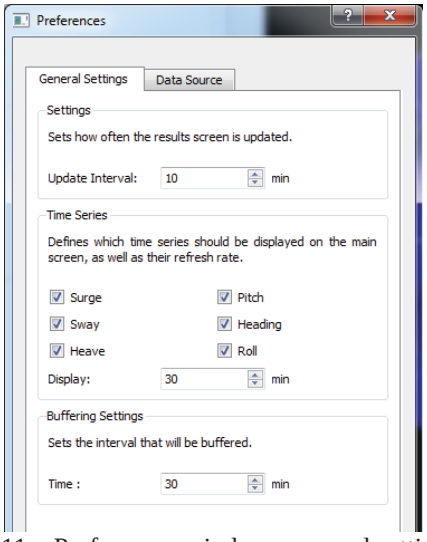

Figure 11 – Preferences window - general settings tab

VALIDATION RESULTS

A long-term campaign is being carried out in order to validate the wave estimation software. The system is installed in a spread-moored FPSO in Campos Basin, Brazil, since July/2011.

The main data of the FPSO is given in Table 1.

Table 1 VLCC-FPSO main properties

Loading Condition	**Full**	**Interm.**	**Ballast**
Length Overall Lpp (m)	337.0		
Beam B (m)	54.0		
Draft T (m)	21.0	14.3	8.0
Displacement (ton)	311335	205348	109863
Rxx/B (%)	35.57	36.26	38.15
Ryy/Lpp (%)	25.23	25.71	29.26
Displ. Ball MTon	25.54	25.89	29.27

The IMU is installed in the platform control room, near the bridge. So, it measures the motions of a point in the stern part of the platform, and not of the center of gravity (CG). It would be possible to make a lever arm compensation, transferring the measuring point to the CG. However, since it is more than 100m away from that point, small misalignments and angle measuring errors may cause very large inaccurate estimation of CG motion.

The adopted solution was to transfer the motion to the reference point, located in the same longitudinal position of the IMU, with the same height of the CG. The lever arm in this case is much smaller than 100m, giving rise to smaller transferring errors. Furthermore, this reference point has no influence of the roll motion, that should be avoided. So, the RAO´s of the platform were calculated in the reference point, and the wave estimation algorithm was applied considering this same point. Figure 12 illustrates the reference point definition.

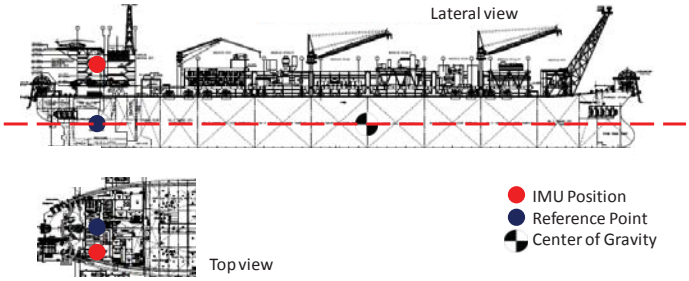

Figure 12 – Measuring reference point definition

The wave data from National Ocean and Atmospheric Administration (NOAA [13]) is being used as a reference for comparison with the spectrum obtained by the wave estimation software. Some illustrative results will be presented in this section.

Data will be presented as bar graphs, containing statistical parameters such as significant height and peak period. Those graphs have a period of 9 days. A polar graph, in which the circles represent the wave-frequency and the direction indicates

where the wave component *goes to* (convention adopted by [13]), will also be presented for a qualitative comparison.

1. Period from 08/17/2011 to 08/25/2011

According to data provided by [13], during the period from 08/17/2011 to 08/25/2011 a bi-modal sea-state shown in Figure 13 and Figure 14 was estimated in the Campos Basin.

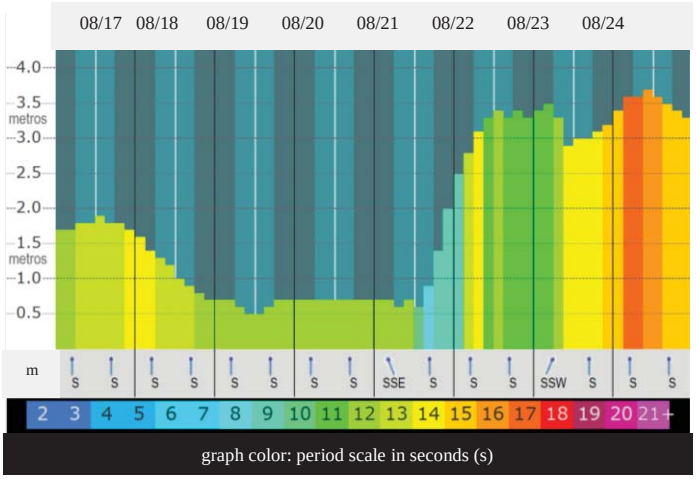

Figure 13 - Significant Height for S/SE waves in Campos Basin from 08/17/2011 to 08/25/2011 [13]

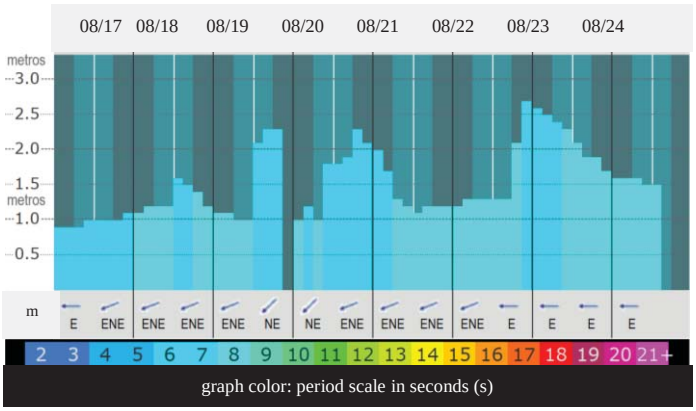

Figure 14 – Significant Height for NE/SE waves in Campos Basin from 08/17/2011 to 08/25/2011 [13]

During the same period, the wave estimation software, with data obtained from FPSO in the Campos Basin, generated the results of Figures 15, 16 and 17.

According to NOAA results, during this period two main wave systems were present: one from S/SE (Figure 13) with a larger peak period and one from NE/SE (Figure 14) with a peak period that fluctuates around 8s. Due to the FPSO dynamics the larger peak period waves are expected to be better estimated, fact that is indeed verified if the estimated peak period graph (Figure 16) is observed. Except for a small time around 08/21, all the estimated periods are consistent with the S/SE waves.

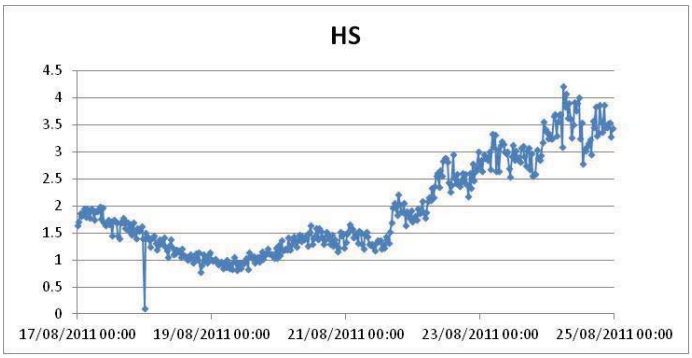

Figure 15- Spectrum's estimated significant height for period from 08/17/2011 to 08/25/2011

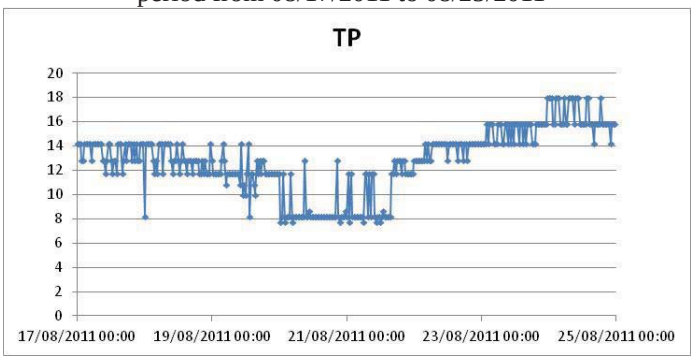

Figure 16 - Spectrum's estimated peak period for period from 08/17/2011 to 08/25/2011

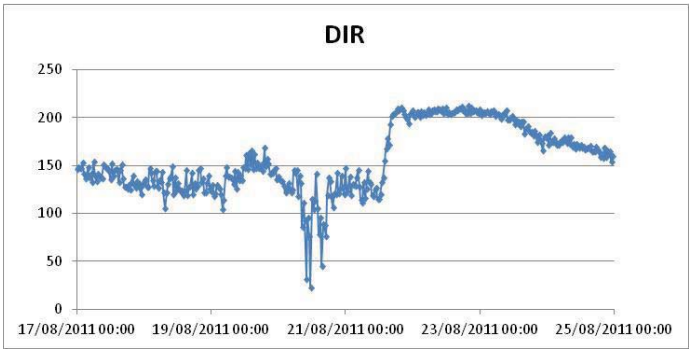

Figure 17 - Spectrum's estimated global direction for period from 08/17/2011 to 08/25/2011

The small period around 08/21 with an estimated peak period of 8s is explained by the NE/SE wave. During this period the significant wave height of the S/SE wave was very low (around 0.5m) while the NE/SE wave had a significant height around 1.3m. In that situation, the influence of the NE/SE wave was dominant.

The estimated global direction graph (Figure 17) can be divided into three periods. The first one starts at 08/17 and ends at 08/20 and shows a direction around SE (135^{o}), which is a mean direction between the ENE wave and the S wave present at this period. The estimated wave polar plot Figure 18a shows these two wave components.

The second period is around the day 08/21, which has an estimated direction close to East and has the same period of the

peak period graph with a higher influence of the NE/SE wave. The estimated wave polar plot Figure 18b shows that in this case the S wave component is in fact weaker.

Finally, the third period starts around the day 08/22 and is consistent with the S/SE wave direction (see also Figure 18c). During this period the S/SE peak period was very high (up to 18s). Because of that its influence in the estimated wave was almost total explaining the correlation founded in both the estimated global direction and the direction obtained by [13].

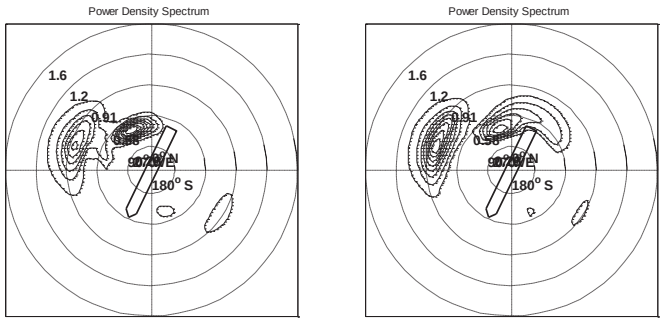

(a) 19-08-2011 (b) 21-08-2011

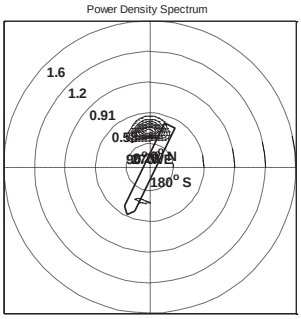

(c) 24-08-2011

Figure 18 - Polar graph generated by wave estimation software (scale in rad/s)

The estimated significant wave height (Figure 15) also has a shape very similar to the S/SE plot (Figure 13), however the values are a little higher for the estimated wave. This fact is explained by the presence of the NE/SE wave. Due to its small period its influence in the estimated wave is less significant than the S/SE but is sufficient to increase the total estimated significant height.

2. Period from 09/01/2011 to 09/09/2011

Based on the data provided by [13], the sea-state was estimated at the Campos Basin during the period from 09/19/2011 to 09/26/2011 (see Figure 19). Only one modal component is presented, since the second one presents a very small significant height (less than 0.5m).

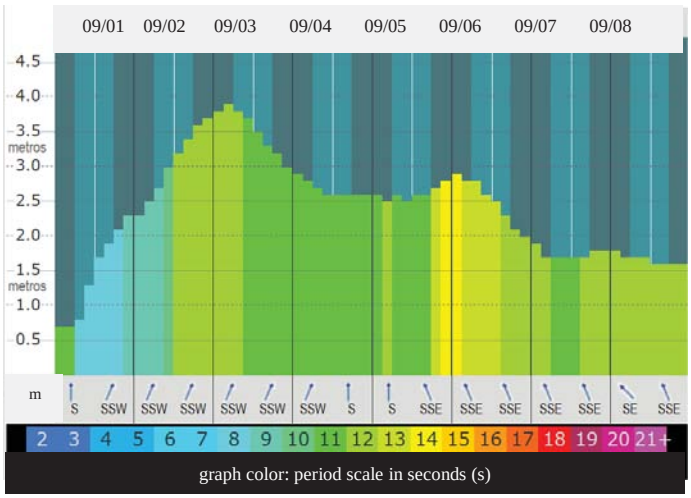

Figure 19 - Southeast South-Southwest waves in Campos Basin during period from 09/19/2011 to 09/26/2011 [13]

During the same period the wave estimation software, with data obtained from FPSO in the Campos Basin, generated the results presented in Figures 20 to 22.

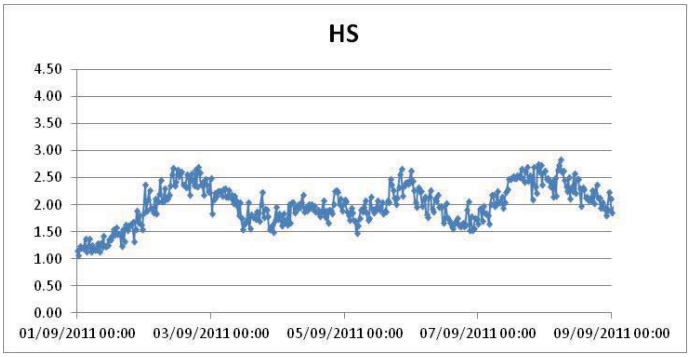

Figure 20- Spectrum's estimated significant height for period from 09/01/2011 to 09/09/2011

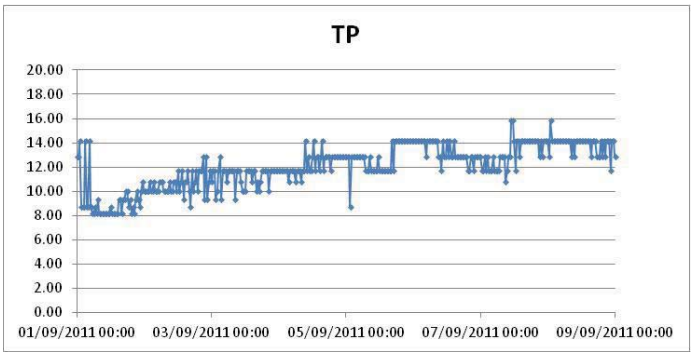

Figure 21 - Spectrum's estimated peak period for period from 09/01/2011 to 09/09/2011

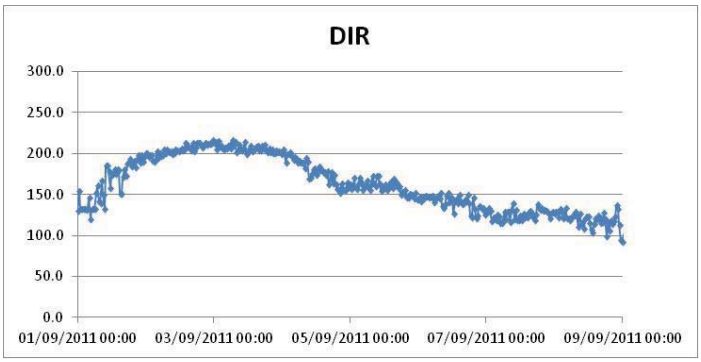

Figure 22 - Spectrum's estimated global direction for period from 09/01/2011 to 09/09/2011

As in the previous analysis, the estimated significant height plot (Figure 20) has a shape very similar to the Southeast South-Southwest waves, but for this period the significant height values are smaller than the ones estimated by [13]. This behavior can be explained by the smaller period of these waves (most part bellow 12s), and some wave spectrum energy may be lost in the estimation process, due to the dynamics of the FPSO. The estimated peak period (Figure 21) and direction plots (Figure 22) are consistent to the estimated by [13].

Looking deeper into some individual estimates, the spectrum polar graph obtained by the wave estimation software is shown in Figure 23.

Comparing to Figure 24 (NOAA) it is easy to verify that the shapes from both are very similar. The estimated spectrum has a significant height of 2.1m, a 10s peak period and a global direction of 17° with respect to North.

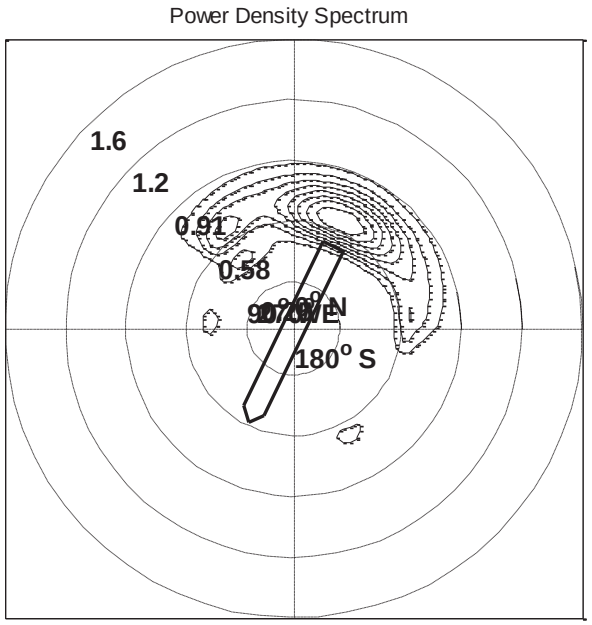

Figure 23 - Polar graph generated by wave estimation software at 09/02/2011 01:30AM (scale in rad/s)

The wave sea forecast obtained from NOAA (Figure 24) shows a spectrum with a main energy peak with a significant height of 2.8m, a 9s peak period and a global direction of 21°, which are also very similar to the estimated values. The second energy peak has a significant height smaller than 0.5m.

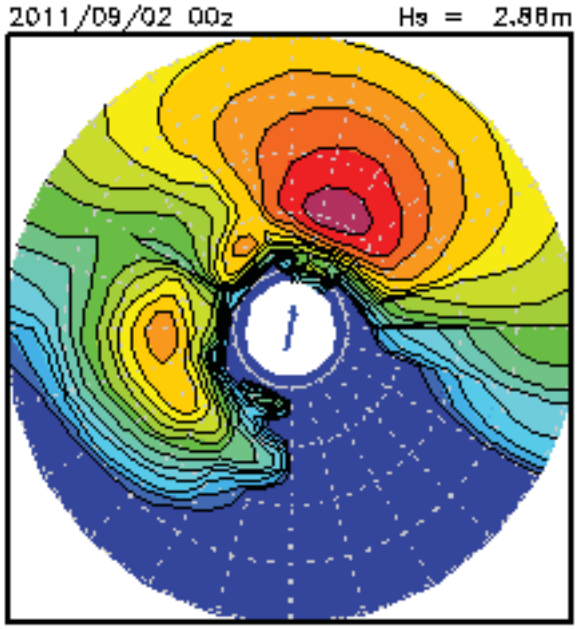

Figure 24 - Wave forecast for day 09/02/2011 at 12:00AM [13]

As could be observed in the previous estimation, the same behavior is verified in the following analysis. Figure 25 shows the estimated wave spectrum for 09/05/2011 with a significant height of 2.1m, a peak period of 12.1s and a global direction of 342°.

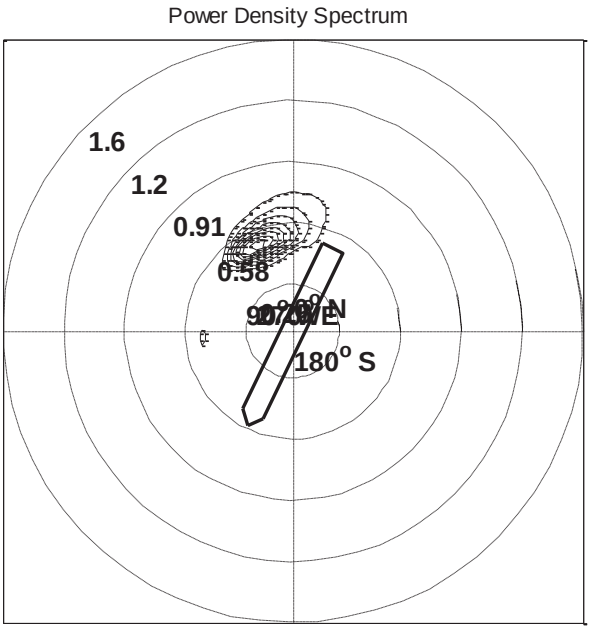

Figure 25 - Polar graph generated by wave estimation software at 09/05/2011 07:30AM (scale in rad/s)

The wave forecast for the same period (Figure 26) shows a spectrum with a main energy peak with a significant height of 1.9m, a 12.1s peak period and a global direction of 343°. As in the previous polar graph the second energy peak has a significant height smaller than 0.5m.

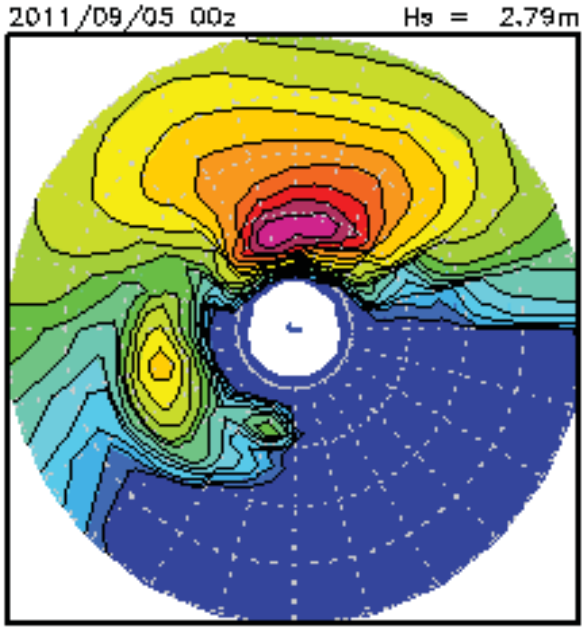

Figure 26 - Wave forecast for day 09/05/2011 at 12:00AM [13]

Another interesting case is the spectrum estimated for 09/05/2011 at midnight. As can be noticed in Figure 27, there is one energy peak with a significant height of 1.9m, a 11.7s peak period and a global direction of 308°.

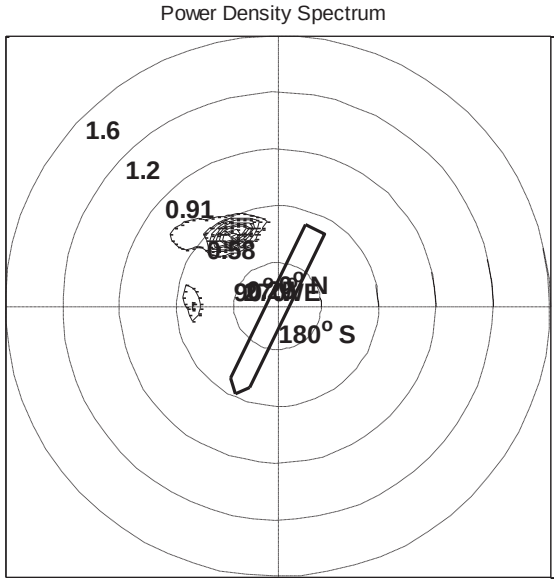

Figure 27 - Polar graph generated by wave estimation software at 09/07/2011 12:30AM (scale in rad/s)

The wave forecast for the same period (Figure 28) shows a spectrum with two main energy peaks, one with a significant height of 2m, a 12s peak period and a global direction of 336°. This energy peak was well estimated by the wave estimation software. The other energy peak, despite its spread, has a significant height of only 0.3m, a 7.5s peak period and a global direction of 260°. The later peak was not captured by the estimation algorithm because of its low energy and period.

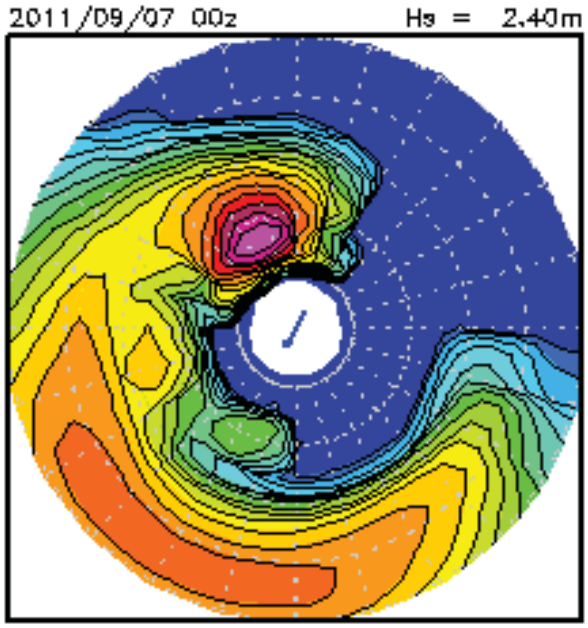

Figure 28 - Wave forecast for day 09/07/2011 at 12:00AM [13]

CONCLUSIONS

The paper presented the development, installation and initial tests of a system for wave spectra estimation from the measurements of the first order motions of a moored VLCC-FPSO located in Campos Basin, Brazil.

The software is integrated with the automation system of the platform, and is able to estimate the wave spectrum two times per hour. A Graphical User Interface was developed, to configure all the parameters of the estimation software, to display the estimated wave spectrum and statistical parameters and to recover the results from previous estimations.

Results from an on-going field campaign were compared to the wave data estimations provided by NOAA. As expected, the results indicated that the system could estimate with good accuracy the wave components with periods higher than 12s, due to the slow dynamic response of the VLCC. For wave components with peak periods between 8s~12s, the average direction and period were obtained with a quite reasonable level of accuracy, although with some energy loss, resulting in smaller wave height. This was already expected, as a consequence of the vessel acting as a filter, not responding to high frequency wave components. Despite the good results

obtained so far, a more comprehensive analysis of the system performance will be possible in the near future, as the monitoring campaign goes on. Also expected in the continuation of this research project is the comparison by means of additional sensors, such as wave radars or buoys.

ACKNOWLEDGMENTS

Authors gratefully acknowledge Petrobras for supporting the research project and providing the funds that made this campaign possible. Special thanks are offered to Dr. Vinícius L.F.Matos for the technical contribution. Authors also acknowledge CNPq, the Brazilian National Research Council, for research-grants.

REFERENCES

[1] Iseki, T., and Ohtsu, K., 2000, "Bayesian estimation of directional wave spectra based on ship motions", Control Engineering Practice, 8, pp.215-219.

[2] Nielsen, U.D., 2008, "Introducing two hyperparameters in Bayesian estimation of wave spectra". Probabilistic Engineering Mechanics, 23, pp. 84-94.

[3] Simos A.N., Tannuri, E.A., Sparano, J.V., Matos, V.L.F., 2010, "Estimating wave spectra from the motions of moored vessels: Experimental validation". Applied Ocean Research 32, pp.191-208.

[4] Tannuri, E. A., Simos, A.N., Sparano, J.V., Cruz, J. J., 2003, "Estimating Directional Wave Spectrum Based On Stationary Ship Motion Measurements". Applied Ocean Research, v. 25, pp. 243-261.

[5] Simos, A.N., Sparano, J.V., Tannuri, E. A., Matos, V. L. F., 2009, "Directional Wave Spectrum Estimation Based on a Vessel 1st Order Motions: Field Results". International Journal of Offshore and Polar Engineering, v. 19, pp. 81-89.

[6] Akaike, H., 1980, "Likelihood and Bayes Procedure'" in Bernardo, J.M., de Groot, M.H., Lindley, D.U. and Smith, A.F.M. Bayesian Statistics, Valencia: University Press.

[7] Nielsen U.D., 2005, "Estimation of directional wave spectra from measured ship responses", Ph.D. thesis. Section of Coastal, Maritime and Structural Engineering, Department of Mechanical Engineering, Technical University of Denmark.

[8] Iseki, T., 2011, "A study on Akaike's Bayesian information criterion in wave estimation", 30th International Conference on Ocean, Offshore and Arctic Engineering, Rotterdam, The Netherlands, pp.103-109.

[9] Iseki, T., and Nielsen, U.D., 2010, "The wave buoy analogy - Analysis of synthetic data by Bayesian modelling", 29th International Conference on Ocean, Offshore and Arctic Engineering, Shanghai, China, pp. 301-310.

[10] Bispo, I. B. S., Simos, A. N., Tannuri E.A., and Da Cruz, J. J., 2012. "Motion-based wave estimation by a Bayesian inference method: a procedure for pre-defining the hyperparameters", submitted to ISOPE.

[11] Piscopia, R., Panizzo, A. and De Girolamo, P., 2004, "An efficient method to identify cross-sea states from wave measurements", Coastal Engineering, 13 September, pp. 941-965.

[12] Hanson, J.L., and Phillips, O.M., Automated Analysis of Ocean Surface Directional Wave Spectra, Journal of Atmospheric and Oceanic T8chnology, 18 February, pp. 277-293.

[12] The HDF Group, 2012, HDF5, Available at <http://www.hdfgroup.org/HDF5/> Access: 01/04/2012.

[13] NOAA, 2012, National Ocean and Atmospheric Administration, Available at < http://polar.ncep.noaa.gov/waves /viewer.shtml?-multi_1-atlantic- >

